



# Effect of Cu addition on the GFA, structure and properties of Fe-Co-based alloy

**S. Lesz<sup>a,\*</sup>, R. Babilas<sup>a</sup>, M. Dośpiał<sup>b</sup>, R. Nowosielski<sup>a</sup>**

<sup>a</sup> Institute of Engineering Materials and Biomaterials, Institute of Engineering Materials and Biomaterials, Silesian University of Technology, ul. Konarskiego 18a, 44-100 Gliwice, Poland

<sup>b</sup> Institute of Physics, Faculty of Materials Processing Technology and Applied Physics, Czestochowa University of Technology, Al. Armii Krajowej 19, 42-200 Częstochowa, Poland

\* Corresponding e-mail address: sabina.lesz@polsl.pl

Received 27.03.2012; published in revised form 01.06.2012

## ABSTRACT

**Purpose:** The aim of the paper was investigation of the effect of Cu addition on GFA (Glass Forming Ability), structure, magnetic and mechanical properties of amorphous Fe-Co-B-Si-Nb alloy.

**Design/methodology/approach:** The following experimental techniques were used: differential thermal analysis (DTA), transmission electron microscopy (TEM) and X-ray diffraction (XRD) method, measurements of magnetic properties (VSM method), Vickers microhardness (HV).

**Findings:** It was shown that when Cu is added to the Fe-Co-based alloy, increase of the GFA and change of the magnetic properties was obtained.

**Research limitations/implications:** The results can give more details to understand the relationship between structure, magnetic and mechanical properties. Thus can be useful for practical application of these alloys.

**Practical implications:** The  $(\text{Fe}_{36}\text{Co}_{36}\text{B}_{19}\text{Si}_5\text{Nb}_4)_{100-x}\text{Cu}_x$  ( $x=0$  and  $0.6$ ) metallic glasses due to their excellent soft magnetic properties have

shown great industrial value for commercial application. Many products consisting of these kinds of metallic glasses have been widely used, for example anti-theft labels, precision sensor material, and high efficient magnetic transformers in electronic industry.

**Originality/value:** The applied investigation methods are suitable to determine the changes of GFA and structure combined with magnetic and mechanical properties of  $(\text{Fe}_{36}\text{Co}_{36}\text{B}_{19}\text{Si}_5\text{Nb}_4)_{100-x}\text{Cu}_x$  ( $x=0$  and  $0.6$ ) metallic glasses.

**Keywords:** Amorphous materials; Magnetic properties; Microhardness; DTA; XRD; TEM method; GFA (glass forming ability)

**Reference to this paper should be given in the following way:**

S. Lesz, R. Babilas, M. Dośpiał, R. Nowosielski, Effect of Cu addition on the GFA, structure and properties of Fe-Co-based alloy, Archives of Materials Science and Engineering 55/2 (2012) 70-77.

## PROPERTIES

### 1. Introduction

Fe-Co-based metallic glasses, especially bulk metallic glasses (BMGs) have attracted extensive interest in recent years for

applications as magnetic and structural materials due to their excellent magnetic and mechanical properties [1-24].

Relatively poor glass forming ability (GFA) of Fe-based metallic glasses (compared to many other metallic glasses, e.g. Pd-based) substantially limits size, and thus the applications of

Fe-based metallic glasses. For this reason extensive efforts have been carried out to improve the GFA of metallic materials and understand the mechanism of effects of various factors on the formation, crystallization, thermal stability and property of metallic glasses [1-11, 13-22].

Recently,  $[(\text{Fe}_x\text{Co}_{1-x})_{0.75}\text{B}_{0.2}\text{Si}_{0.05}]_{96}\text{Nb}_4$  ( $x=0.1-0.5$  at.%) BMGs were produced which exhibit high GFA as well as good soft magnetic properties (saturation magnetization  $I_s \approx 1$  T, permeability  $\mu \approx 12000$ , coercive force  $H_c \approx 2$  A/m) and mechanical properties (fracture strength  $\sigma \approx 4000$  MPa and plastic strain  $\varepsilon_p \approx 0.002$ ) [3,5,7]. With the aim of searching for Fe-based BMGs with high GFA and excellent magnetic and mechanical properties, the effect of the replacement of Fe by Co and alloying addition have been investigated. The partial substitution of Co atoms for Fe atoms in Fe-based nanocrystalline alloys increases considerably the soft magnetic properties but remarkably increases the cost of the materials. An important role in improving the soft magnetic properties plays the substitution of Cu for Fe-based alloys [14]. Very recently the effect of Cu addition on the GFA of  $(\text{Fe}_{36}\text{Co}_{36}\text{B}_{19.2}\text{Si}_{4.8}\text{Nb}_4)_{100-x}\text{Cu}_x$  ( $x=0, 0.5, 0.6, \text{ and } 1.0$  at.%) alloy was studied [4,14]. It is believed that some small additions of Cu may promote the nanocrystallization due to its positive heat of mixing with Fe, Co and Nb [3]. Subsequently, the magnetic properties, as well as the mechanical properties, may become better. It was found that the addition of Cu can be positive on the GFA of a Fe-Co-based alloy [4].

In this paper  $\text{Fe}_{36}\text{Co}_{36}\text{B}_{19}\text{Si}_5\text{Nb}_4$  metallic glass were chosen for investigation as the base alloy because it has best GFA among the Fe-Co-based alloys reported by Shen et al. [2,7,20]. Further investigations exhibit that among the  $(\text{Fe}_{36}\text{Co}_{36}\text{B}_{19.2}\text{Si}_{4.8}\text{Nb}_4)_{100-x}\text{Cu}_x$  ( $x=0, 0.5, 0.6, \text{ and } 1.0$  at.%) alloy only copper addition equal 0.6 guarantees only one endothermic peak upon melting, which implies that the addition of Cu depressed the precipitation of the primary phase. This concentrations of Cu allow to obtain good mechanical properties, too [4].

In the present paper we have studied the effect of small amounts of Cu, which are well known to have a large negative mixing enthalpy with Fe [4], and non-solubility into Fe in solid [11] on the on structure, GFA and magnetic properties of  $(\text{Fe}_{36}\text{Co}_{36}\text{B}_{19}\text{Si}_5\text{Nb}_4)_{100-x}\text{Cu}_x$  ( $x=0$  and 0.6 at.%) metallic glasses. However, many works were dedicated to the results of thermal and mechanical properties investigations, there have been no published data referring to magnetic properties of these alloys with copper addition. In particular interesting is the relationship between structure combined with magnetic and mechanical properties.

## 2. Experiments

Master alloy ingots with the nominal composition of  $(\text{Fe}_{36}\text{Co}_{36}\text{B}_{19}\text{Si}_5\text{Nb}_4)_{100-x}\text{Cu}_x$  (at.%), where  $x=0$  and 0.6 were prepared by induction melting the mixtures of the Fe-B, Fe-Nb, Fe-Si starting industrial alloys and pure Fe, Co, Cu metals under protective argon atmosphere. For this procedure, induction was preferred in order to assure a good homogeneity of the entire master alloy. The master alloys were remelted in quartz tube. From the master alloys, ribbons with thickness of 0.07 and 0.12 mm and width of 2.3 mm were produced by melt-spinning technique on a copper wheel in inert argon atmosphere.

The structure of the as-cast alloys was identified by X-ray diffraction (XRD, X-Pert PRO MP) using filtered Co-K $\alpha$  radiation ( $\lambda=0.17888$  nm) in Bragg-Brentano geometry. In order to conduct structural study, the electron microscope (TEM, TESLA BS 540) in the range of 52000 $\times$  to 150000 $\times$  magnitude was used.

Thermal properties (liquidus -  $T_l$  and solidus -  $T_s$  temperatures of the pre-alloyed ingots (as well as the base alloy and the alloy with 0.6 at.% copper addition) were determined from the differential thermal analysis (DSC 404 C Pegasus, NETZSCH) at the heating and cooling rate of 0.333 K/s under the purified argon atmosphere [25].

Magnetic hysteresis loops were measured with a vibrating sample magnetometer (VSM) under an applied field up to 1 T. Magnetic properties of saturation magnetization -  $I_s$  and coercive force -  $H_c$  were determined from achieved magnetic hysteresis loops. Hysteresis loops, recorded using a computer controlled DC hysteresis loop tracer, were used to obtain hysteresis parameters.

For samples, the relative magnetic permeability (Maxwell-Wien bridge, frequency 1 kHz, magnetic field 0.5 A/m) at room temperature were obtained.

The measurements of magnetic permeability -  $\mu_i$  (at force  $H \approx 0.5$  A/m and frequency  $f \approx 1$  kHz) and the intensity of magnetic after effect -  $\Delta\mu/\mu(t_i)$  ( $\Delta\mu = \mu(t_1=30 \text{ s}) - \mu(t_2=1800 \text{ s})$ ), where  $\mu$  is the initial magnetic permeability measured at time -  $t$  after demagnetisation, have been done. The investigations of ribbons were performed with the use of automatic device for measurements magnetic permeability [23,24].

Mechanical properties (microhardness) was measured with a use of the Vickers hardness tester FUTURE-TECH FM-700 under the load of 0.49N (50G) [26]. The microhardness was measured on the shining surface of ribbons according to pattern presented in Fig.1.

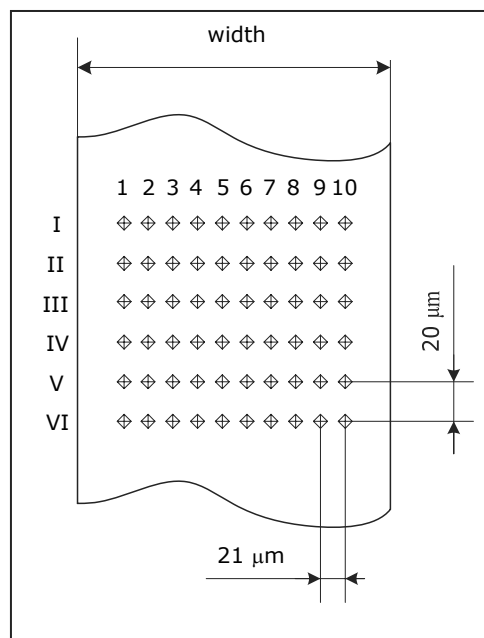


Fig. 1. The pattern of microhardness measurements

### 3. Results and discussion

In order to predict the effect of small addition of element as Cu to the base (mother) alloy, the structure, magnetic and mechanical properties were investigated.

Fig. 2a,b shows XRD patterns for these cast alloy ribbons. Only broad peak without any crystalline peaks can be seen for the all of ribbons as well as  $\text{Fe}_{36.00}\text{Co}_{36.00}\text{B}_{19.00}\text{Si}_5\text{Nb}_4$  and  $\text{Fe}_{35.75}\text{Co}_{35.75}\text{B}_{18.90}\text{Si}_5\text{Nb}_4\text{Cu}_{0.6}$ .

Obtained results of structural studies performed by XRD are corresponding with the TEM micrograph. The diffraction pattern taken from the small region consists only of halo rings, and no appreciable reflection spots of crystalline phases are seen (Figs. 3-6). It was found from the obtained results of structural studies that the structure of every sample is amorphous.

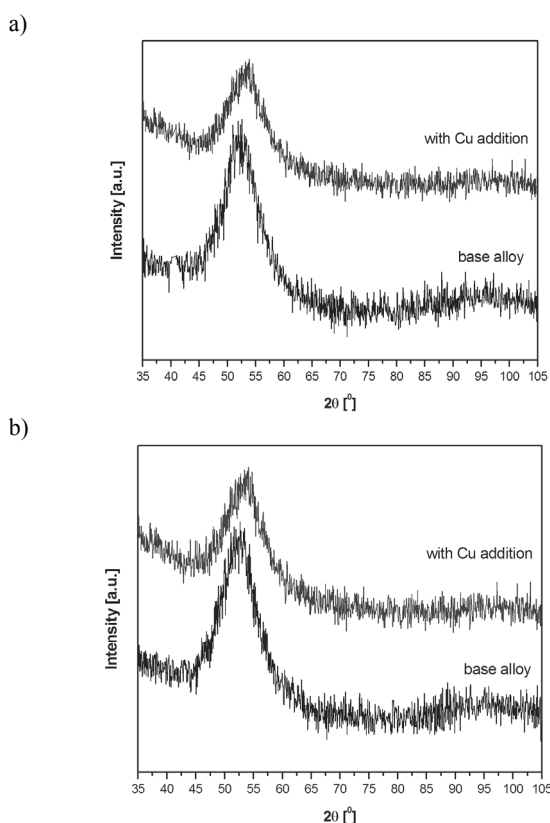


Fig. 2. X-ray diffraction pattern of the  $\text{Fe}_{36.00}\text{Co}_{36.00}\text{B}_{19.00}\text{Si}_5\text{Nb}_4$  and  $\text{Fe}_{35.75}\text{Co}_{35.75}\text{B}_{18.90}\text{Si}_5\text{Nb}_4\text{Cu}_{0.6}$  ribbons with thickness of 0.07 mm (a) and ribbons with thickness of 0.12 mm (b)

From DTA, a course of eutectic transformation was determined for a base alloy containing 0.6at% Cu.

The thermal properties of the pre-alloyed ingots base alloy and the alloy with 0.6 at.% Cu addition upon heating measured by DTA are presented on Fig. 7. On heating, melting requires an input of heat and the peak is endothermic. The base alloy and Cu added alloy present clearly two endothermic peaks. The first peak for base alloy begins near the eutectic (melting) point - 1312 K. For alloy with Cu addition the onset of melting occurs at the eutectic temperature, 1305 K.

Fig. 8 shows thermal properties of the pre-alloyed ingots base alloy and the alloy with 0.6% Cu addition upon cooling measured by DTA. For the base alloy two peaks are clearly shown (Fig. 8). The first peak corresponds to the eutectic temperature (1294 K) and the maximum signal of the second peak occurs near the liquidus (1393 K). The reason the maximum signal of the second peak is associated with the liquidus temperature will be discussed in [25]. For the alloy with 0.6%at. Cu addition only one major peak is observed ( $T_{peak}=1282$  K). For these alloy the onset of melting occurs at 1266 K and end at 1303 K. This peak is undoubtedly the eutectic transformation temperature. Y. Jia reported that the copper addition to the base alloy depresses the possibility of the precipitation of the competing phase and thus improved the GFA of the base alloy [4]. The Cu addition to the base alloy can approaching the alloy composition to a eutectic point, leading to increase the GFA. The GFA of an alloy is composition - dependent [4,14].

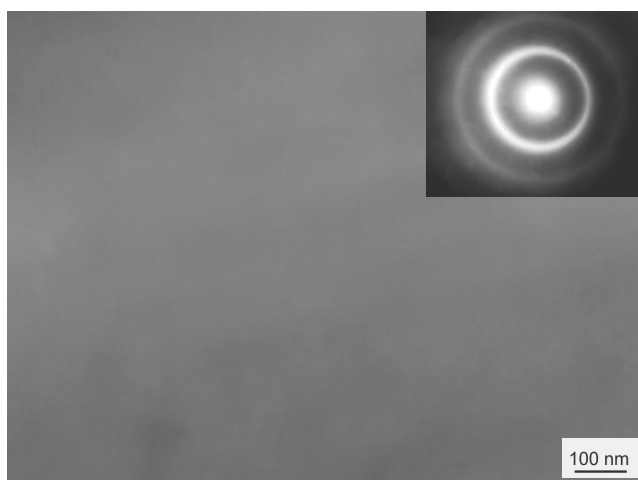


Fig. 3. TEM micrograph and electron diffraction pattern of selected area of as-cast  $\text{Fe}_{36.00}\text{Co}_{36.00}\text{B}_{19.00}\text{Si}_5\text{Nb}_4$  ribbons with thickness of 0.07 mm

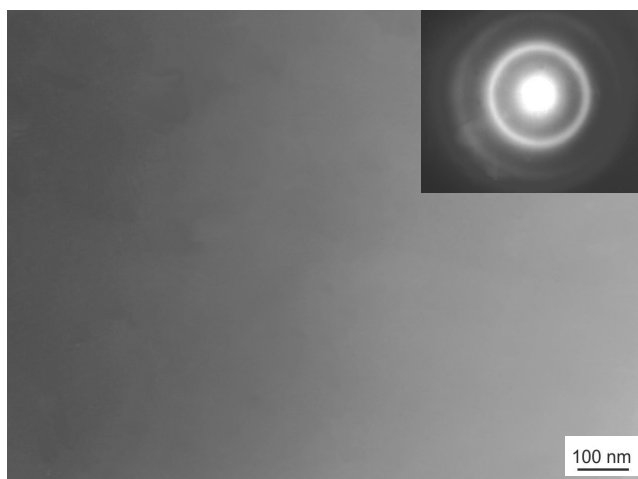


Fig. 4. TEM micrograph and electron diffraction pattern of selected area of as-cast  $\text{Fe}_{35.75}\text{Co}_{35.75}\text{B}_{18.90}\text{Si}_5\text{Nb}_4\text{Cu}_{0.6}$  ribbons with thickness of 0.07 mm

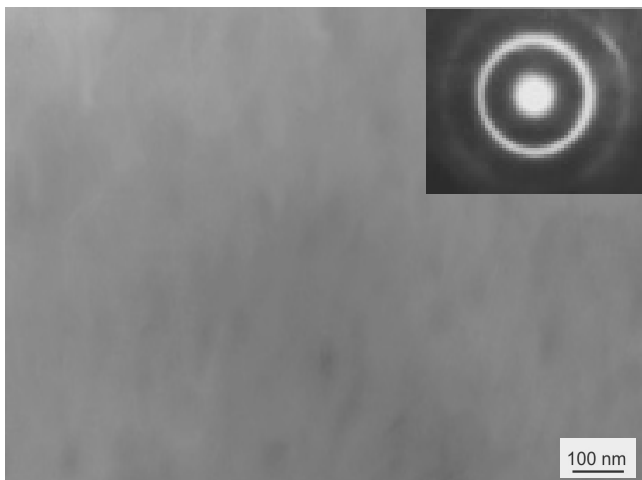


Fig. 5. TEM micrograph and electron diffraction pattern of selected area of as-cast  $\text{Fe}_{36.00}\text{Co}_{36.00}\text{B}_{19.00}\text{Si}_5\text{Nb}_4$  ribbons with thickness of 0.12 mm

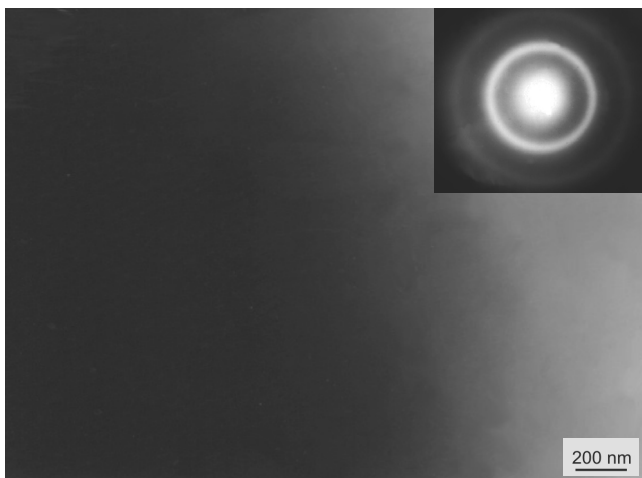


Fig. 6. TEM micrograph and electron diffraction pattern of selected area of as-cast  $\text{Fe}_{35.75}\text{Co}_{35.75}\text{B}_{18.90}\text{Si}_5\text{Nb}_4\text{Cu}_{0.6}$  ribbons with thickness of 0.12 mm

The results of magnetic properties measurements of the investigated ribbons of the  $(\text{Fe}_{36}\text{Co}_{36}\text{B}_{19}\text{Si}_5\text{Nb}_4)_{100-x}\text{Cu}_x$ , ( $x=0$  and 0.6 at.%) alloys have been presented in the Table 1.

The values of saturation magnetization -  $I_s$  and coercivity -  $H_c$  obtained from the VSM curves are plotted in Fig. 9 a,b and Fig. 10 a, b.

The coercivity -  $H_c$  of the metallic glasses increases from 7.2 A/m ( $\text{Fe}_{36.00}\text{Co}_{36.00}\text{B}_{19.00}\text{Si}_5\text{Nb}_4$  ribbons with thickness of 0.07 mm) to 31.0 A/m with Cu addition (Fig. 9a, b). Similar coercivity increase has been found in  $\text{Fe}_{36.00}\text{Co}_{36.00}\text{B}_{19.00}\text{Si}_5\text{Nb}_4$  ribbons with thickness of 0.12 mm with Cu addition (Fig. 10a, b). The highest value of saturation magnetization -  $I_s \approx 1.2$  T have been measured for the  $\text{Fe}_{35.75}\text{Co}_{35.75}\text{B}_{18.90}\text{Si}_5\text{Nb}_4\text{Cu}_{0.6}$  ribbons with thickness of 0.12 mm. The highest value of initial permeability -  $\mu_i \approx 3620$  have been measured for the  $\text{Fe}_{35.75}\text{Co}_{35.75}\text{B}_{18.90}\text{Si}_5\text{Nb}_4\text{Cu}_{0.6}$  ribbons with thickness of 0.07 mm.

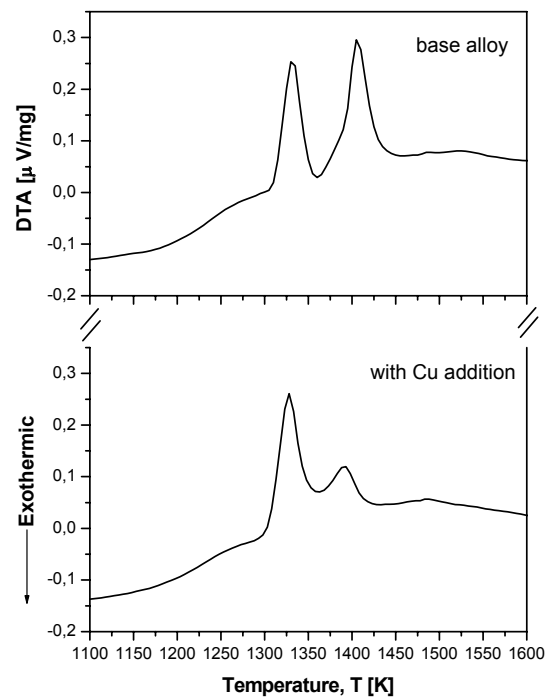


Fig. 7. Differential thermal analysis (DTA) curves of the base master alloy and of the Cu added alloy under the heating rate of 0.333 K/s

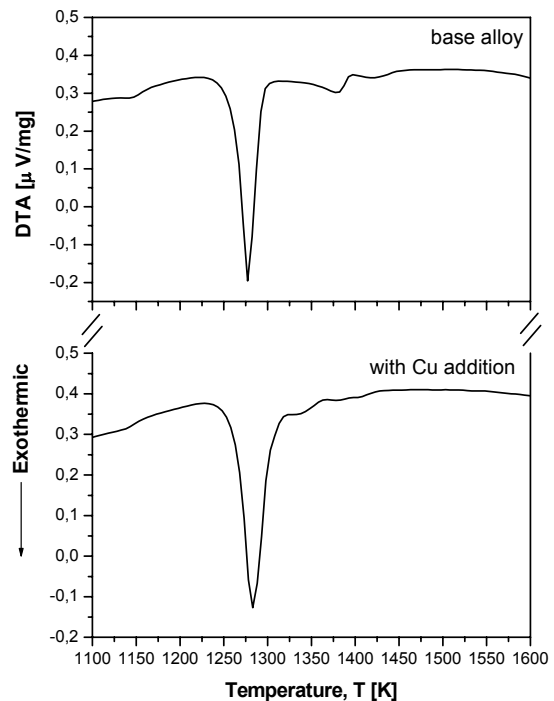


Fig. 8. Differential thermal analysis (DTA) curves of the base master alloy and of the Cu added alloy under the cooling rate of 0.333 K/s

The addition of Cu to the base alloy improved magnetic permeability -  $\mu_i$  and saturation magnetization -  $I_s$  what probably is connected with impurity content. Y. Jia reported that the Cu addition reduces of oxygen content of the alloy [14]. A remarkably higher value of coercivity -  $H_c$  has been measured for the alloy with Cu addition. In the amorphous alloy, the domain walls are free to move due to the low magnetocrystalline anisotropy, resulting in a low  $H_c$ . The lower coercivity -  $H_c$  could be obtained upon heating in order to reduce the stress field in the as-cast amorphous matrix. The addition of Cu to the base alloy extend the crystallization procedure, which provides us a chance to obtain nano-structured material with better soft magnetic property by annealing the alloy avoiding the rapid crystallization of the amorphous precursor [14].

However, when there are crystallites or impurities in the alloy, they can pin the domain walls. This might result in a high coercivity -  $H_c$  [27].

The thinner ribbons have lower values of magnetic after effects ( $\Delta\mu/\mu$ ), than thicker ribbons, what suggests that the casting conditions have influence on microvoids content and thereby on magnetic properties. The microvoids content is often examined

using magnetic after effects ( $\Delta\mu/\mu$ ) measurements. The value of  $\Delta\mu/\mu$  increases with increasing of microvoids into materials [23]. All of the studied samples present in the glassy state ferromagnetism at room temperature and have low coercivity values (Table 1, Fig. 9a, b, Fig. 10a, b), which are the most important requirements for a soft magnetic material.

Results of microhardness measurements of the investigated ribbons with thickness of 0.07 mm and 0.12 mm of the  $(\text{Fe}_{36}\text{Co}_{36}\text{B}_{19}\text{Si}_5\text{Nb}_4)_{100-x}\text{Cu}_x$  ( $x=0$  and 0.6 at.%) alloys have been presented in Tables 2, 3 and 4, 5, respectively.

The results of microhardness measurements points to changeable microhardness of  $(\text{Fe}_{36}\text{Co}_{36}\text{B}_{19}\text{Si}_5\text{Nb}_4)_{100-x}\text{Cu}_x$  ( $x=0$  and 0.6) ribbons with thickness of 0.07 mm and 0.12 mm depended on place of measurements.

The microhardness -  $H_v$  varies between 1413-1789 on the margin of ribbons and 1049-1314 in centre of  $\text{Fe}_{36}\text{Co}_{36}\text{B}_{19}\text{Si}_5\text{Nb}_4$  ribbons (Tables 2, 3). Similarity microhardness -  $H_v$  of  $\text{Fe}_{35.75}\text{Co}_{35.75}\text{B}_{18.90}\text{Si}_5\text{Nb}_4\text{Cu}_{0.6}$  alloy varies between 1524-1789 on the margin of ribbons and 1197-1524 in centre of ribbons (Tables 4, 5). These differences may suggest that process of solidification of amorphous ribbons is different in centre and on the margin and is connected with cooling rate of ribbons during casting.

Table 1.

Magnetic properties ( $\mu_i$  -initial magnetic permeability,  $\Delta\mu/\mu$  - magnetic after effects,  $H_c$  - coercivity,  $I_s$  - saturation magnetization) of  $(\text{Fe}_{36}\text{Co}_{36}\text{B}_{19}\text{Si}_5\text{Nb}_4)_{100-x}\text{Cu}_x$  ( $x=0$  and 0.6 at.%) ribbons with thickness of 0.07 mm and 0.12 mm

Composition of alloys [at. %]	Thickness of ribbons [mm]	Magnetic properties			
		$\mu_i$	$\Delta\mu/\mu$ [%]	$H_c$ [A/m]	$I_s$ [T]
$\text{Fe}_{36.00}\text{Co}_{36.00}\text{B}_{19.00}\text{Si}_5\text{Nb}_4$	0.07	3000	5.0	7.2	0.6
$\text{Fe}_{35.75}\text{Co}_{35.75}\text{B}_{18.90}\text{Si}_5\text{Nb}_4\text{Cu}_{0.6}$	0.07	3620	11.0	31.0	1.1
$\text{Fe}_{36.00}\text{Co}_{36.00}\text{B}_{19.00}\text{Si}_5\text{Nb}_4$	0.12	1567	3.6	6.4	0.7
$\text{Fe}_{35.75}\text{Co}_{35.75}\text{B}_{18.90}\text{Si}_5\text{Nb}_4\text{Cu}_{0.6}$	0.12	1980	10.0	49.0	1.2

Table 2.

Results of microhardness measurements (see Fig. 1) of  $\text{Fe}_{36.00}\text{Co}_{36.00}\text{B}_{19.00}\text{Si}_5\text{Nb}_4$  ribbons with thickness of 0.07 mm

No.	1	2	3	4	5	6	7	8	9	10
I	1648	1648	1413	1524	1197	1648	1413	1648	1648	1648
II	1648	1413	1524	1413	1314	1197	1314	1413	1524	1789
III	1524	1413	1413	1413	1197	1197	1314	1524	1648	1648
IV	1413	1648	1648	1413	1314	1314	1413	1524	1789	1789
V	1648	1413	1524	1413	1197	1314	1314	1413	1648	1648
VI	1524	1413	1413	1524	1314	1197	1314	1524	1524	1648

Table 3.

Results of microhardness measurements (see Fig. 1) of  $\text{Fe}_{35.75}\text{Co}_{35.75}\text{B}_{18.90}\text{Si}_5\text{Nb}_4\text{Cu}_{0.6}$  ribbons with thickness of 0.07 mm

No.	1	2	3	4	5	6	7	8	9	10
I	1648	1648	1524	1314	1524	1197	1413	1789	1648	1789
II	1648	1648	1524	1413	1314	1314	1524	1789	1789	1648
III	1648	1789	1648	1413	1524	1314	1524	1524	1648	1648
IV	1648	1789	1413	1524	1413	1524	1524	1789	1648	1789
V	1648	1648	1524	1648	1413	1413	1648	1524	1789	1789
VI	1789	1524	1413	1524	1413	1524	1648	1648	1648	1789

Table 4.

Results of microhardness measurements (see Fig. 1) of  $\text{Fe}_{36.00}\text{Co}_{36.00}\text{B}_{19.00}\text{Si}_5\text{Nb}_4$  ribbons with thickness of 0.12 mm

No.	1	2	3	4	5	6	7	8	9	10
I	1648	1413	1314	1413	1197	1413	1524	1789	1648	1648
II	1648	1648	1314	1314	1197	1524	1413	1524	1648	1648
III	1648	1524	1413	1314	1314	1314	1413	1648	1648	1648
IV	1648	1648	1648	1524	1413	1314	1413	1524	1524	1648
V	1648	1648	1524	1314	1413	1524	1413	1648	1648	1648
VI	1648	1648	1648	1413	1314	1413	1413	1648	1648	1648

Table 5.

Results of microhardness measurements (see Fig. 1) of  $\text{Fe}_{35.75}\text{Co}_{35.75}\text{B}_{18.90}\text{Si}_5\text{Nb}_4\text{Cu}_{0.6}$  ribbons with thickness of 0.12 mm

No.	1	2	3	4	5	6	7	8	9	10
I	1648	1789	1524	1314	1314	1197	1524	1524	1648	1648
II	1648	1789	1648	1413	1197	1197	1314	1524	1789	1648
III	1789	1648	1413	1413	1314	1314	1413	1413	1648	1789
IV	1648	1648	1648	1524	1314	1413	1314	1413	1524	1789
V	1789	1648	1524	1524	1413	1197	1197	1314	1648	1524
VI	1648	1524	1648	1314	1314	1413	1314	1413	1648	1789

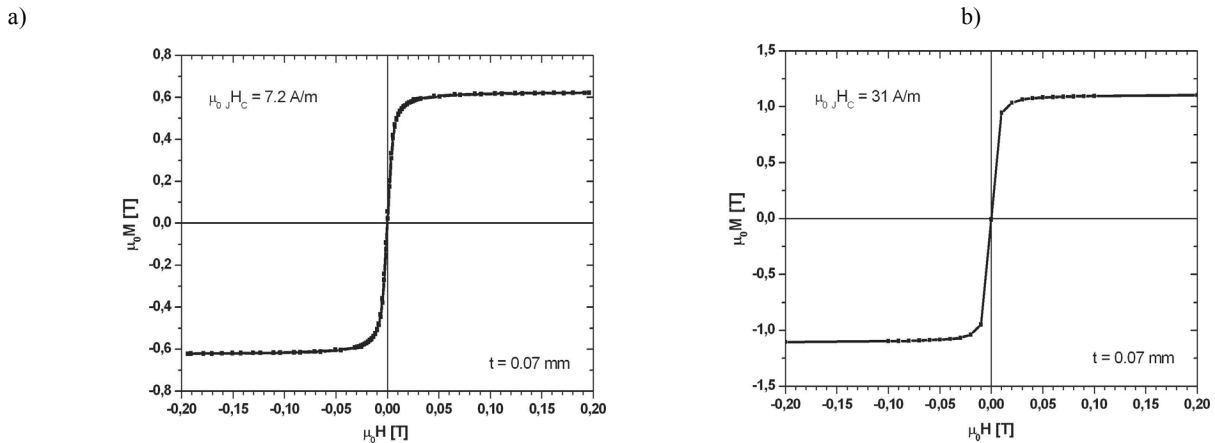


Fig. 9. Room temperature magnetic hysteresis loops measured at a maximum applied field of 0.2 T for  $\text{Fe}_{36.00}\text{Co}_{36.00}\text{B}_{19.00}\text{Si}_5\text{Nb}_4$  (a) and 1 T for  $\text{Fe}_{35.75}\text{Co}_{35.75}\text{B}_{18.90}\text{Si}_5\text{Nb}_4\text{Cu}_{0.6}$  ribbons with thickness of 0.07 mm (b)

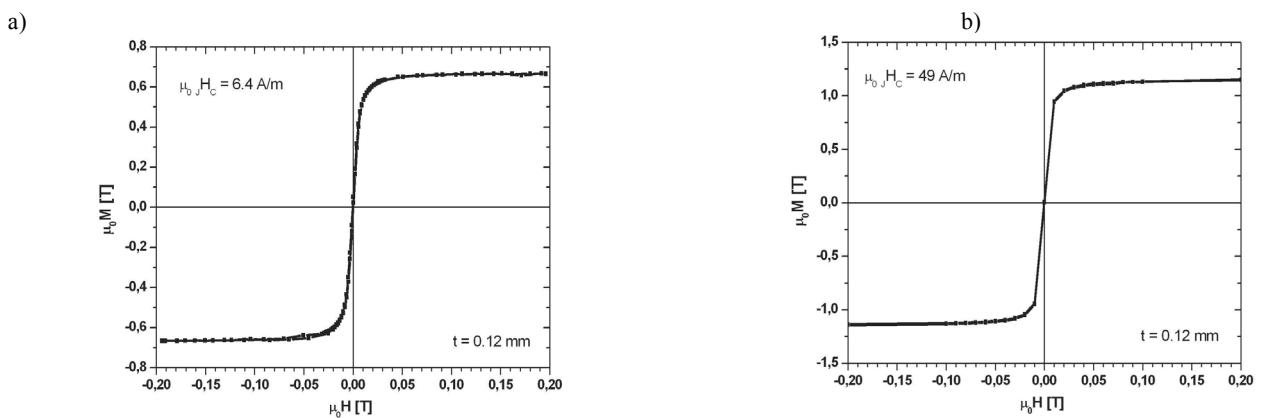


Fig. 10. Room temperature magnetic hysteresis loops measured at a maximum applied field of 0.2 T for  $\text{Fe}_{36.00}\text{Co}_{36.00}\text{B}_{19.00}\text{Si}_5\text{Nb}_4$  (a) and 1 T for  $\text{Fe}_{35.75}\text{Co}_{35.75}\text{B}_{18.90}\text{Si}_5\text{Nb}_4\text{Cu}_{0.6}$  ribbons with thickness of 0.12 mm (b)

## 4. Conclusions

We can state that the structure of the all of ribbons as well as  $\text{Fe}_{36.00}\text{Co}_{36.00}\text{B}_{19.00}\text{Si}_5\text{Nb}_4$  and  $\text{Fe}_{35.75}\text{Co}_{35.75}\text{B}_{18.90}\text{Si}_5\text{Nb}_4\text{Cu}_{0.6}$  alloy is amorphous.

The addition of small amounts of Cu is effective in changing GFA and magnetic properties.

The melting temperature -  $T_m$  remained almost constant for both investigated alloy. Two alloy compositions are at or very close to the eutectics. According to ref. [28], the best metallic glass-forming alloys are at or near deep eutectic composition.

The investigated alloys have good soft magnetic properties. Initial magnetic permeability -  $\mu_i$  and saturation magnetization -  $I_s$  of ribbons of Cu added alloy are better than base alloy. However values of  $H_c$  of copper added alloy considerably exceed values obtained for base alloy.

The successful synthesis of the  $\text{Fe}_{36}\text{Co}_{36}\text{B}_{19}\text{Si}_5\text{Nb}_4$  and  $\text{Fe}_{35.75}\text{Co}_{35.75}\text{B}_{18.90}\text{Si}_5\text{Nb}_4\text{Cu}_{0.6}$  alloy with high GFA and good soft magnetic properties by using starting industrial alloys are encouraging for the future industry applications. In the light of these results, Fe-Co-based alloys can open up a wide range of application by designing the magnetic properties changing geometry, i.e. rods or tubes exploiting the wide possibility that bulk metallic glasses display.

## References

- [1] J. Torrens-Serra, P. Bruna, J. Rodriguez-Viejo, S. Roth, M.T. Clavaguera-Mora, Effect of minor additions on the glass forming ability and magnetic properties of Fe-Nb-B based metallic glasses, *Intermetallics* 18 (2010) 773-780.
- [2] H.J. Sun, L. Li, Y.Z. Fang, J.X. Si, B. L. Shen, Bulk glassy  $(\text{Fe}_{0.474}\text{Co}_{0.474}\text{Nb}_{0.052})_{100-x}(\text{B}_{0.8}\text{Si}_{0.2})_x$  alloys prepared using commercial raw materials, *Journal of Non-Crystalline Solids* 358 (2012) 911-914.
- [3] M. Stoica, R. Li, A. R. Yavari, G. Vaughan, J. Eckert, N. Van Steenberge, D.R. Romera, Thermal stability and magnetic properties of FeCoBSiNb bulk metallic glasses, *Journal of Alloys and Compounds* 504S (2010) S123-S128.
- [4] Y. Jia, S. Zeng, S. Shan, L. Zhang, C. Fan, B. Zhang, Z. Zhan, R. Liu, W. Wang, Effect of copper addition on the glass forming ability of a Fe-Co based alloy, *Journal of Alloys and Compounds* 440 (2007) 113-116.
- [5] A. Inoue, B.L. Shen, C.T. Chang, Fe- and Co-based bulk glassy alloys with ultrahigh strength of over 4000 MPa, *Intermetallics* 14 (2006) 936-944.
- [6] A. Inoue, B. Shen, A. Takeuchi, Fabrication, properties- and applications of bulk glassy alloys in late transition metal-based systems, *Materials Science and Engineering A* 441 (2006) 18-25.
- [7] B. Shen, A. Inoue, Superhigh strength and good soft-magnetic properties of (Fe,Co)-B-Si-Nb bulk glassy alloys with high glass-forming ability, *Applied Physics Letters* 85/21 (2004) 4911-4913.
- [8] S. Lesz, R. Babilas, M. Nabiałek, M. Szota, M. Dośpiał, R. Nowosielski, The characterization of structure, thermal stability and magnetic properties of Fe-Co-B-Si-Nb bulk amorphous and nanocrystalline alloys, *Journal of Alloys and Compounds* 509S (2011) 197-201.
- [9] S. Lesz, Preparation of Fe-Co-based bulk amorphous alloy from high purity and industrial raw materials, *Archives of Materials Science and Engineering* 48/2 (2011) 77-88.
- [10] S. Lesz, R. Nowosielski, Structure and physical properties of Fe-based metallic glasses with Ni and Co addition, *Journal of Achievements in Materials and Manufacturing Engineering* 48/2 (2011) 145-152.
- [11] A. Makino, X. Li, K. Yubuta, C. Chang, T. Kubota, A. Inoue, The effect of Cu on the plasticity of Fe-Si-B-P based bulk metallic glass, *Scripta Materialia* 60 (2009) 277-280.
- [12] Y.Y. Sun, M. Song, X.Z. Liao, Y.H. He, Mechanical properties of a FeCuSiB alloy with amorphous and/or crystalline structures, *Journal of Alloys and Compounds* 509 (2011) 6603-6608.
- [13] Y. Dong, A. Wang, Q. Man, B. Shen,  $(\text{Co}_{1-x}\text{Fe}_x)_{68}\text{B}_{21.9}\text{Si}_{5.1}\text{Nb}_5$  bulk glassy alloys with high glass-forming ability, excellent soft-magnetic properties and superhigh fracture strength, *Intermetallics* 23 (2012) 63- 67.
- [14] S. Lesz, Z. Stokłosa, R. Nowosielski, Influence of copper addition on properties of  $(\text{Fe}_{36}\text{Co}_{36}\text{B}_{19}\text{Si}_5\text{Nb}_4)_{100-x}\text{Cu}_x$  metallic glasses, *Archives of Materials Science and Engineering* 38/1 (2009) 12-18.
- [15] R. Nowosielski, R. Babilas, P. Ochinn, Z. Stokłosa, Thermal and magnetic properties of selected Fe-based metallic glasses, *Archives of Materials Science and Engineering* 30/1 (2008) 13-16.
- [16] R. Babilas, S. Griner, P. Sakiewicz, R. Nowosielski, Structure, thermal and magnetic properties of  $(\text{Fe}_{72}\text{B}_{20}\text{Si}_4\text{Nb}_4)_{100-x}\text{Y}_x$  ( $x = 0,3$ ) metallic glasses, *Journal of Achievements in Materials and Manufacturing Engineering* 44/2 (2011) 140-147.
- [17] R. Babilas, R. Nowosielski, Iron-based bulk amorphous alloys, *Archives of Materials Science and Engineering*, 44/1 (2010) 5-27.
- [18] R. Nowosielski, R. Babilas, Structure and magnetic properties of  $\text{Fe}_{36}\text{Co}_{36}\text{B}_{19}\text{Si}_5\text{Nb}_4$  bulk metallic glasses, *Journal of Achievements in Materials and Manufacturing Engineering* 30/2 (2008) 135-140.
- [19] R. Nowosielski, R. Babilas, Glass-forming ability analysis of selected Fe-based bulk amorphous alloys, *Journal of Achievements in Materials and Manufacturing Engineering* 42 (2010) 66-72.
- [20] B. Shen, C. Chang, A. Inoue, Formation, ductile deformation behavior and soft - magnetic properties of (Fe, Co, Ni)-B-Si-Nb bulk glassy alloys, *Intermetallics* 15 (2007) 9-16.
- [21] C. Suryanarayana, A. Inoue, *Bulk metallic glasses*, CRC Press Taylor & Francis Group Boca Raton, London, New York, 2011.
- [22] R. Babilas, M. Kądziołka-Gawel, R. Nowosielski, Structure studies of Fe-based metallic glasses by Mössbauer spectroscopy method, *Journal of Achievements in Materials and Manufacturing Engineering* 45/1 (2011) 7-12.
- [23] P. Kwapiński, J. Rasek, Z. Stokłosa, G. Badura, B. Kostrubiec, G. Haneczok, Magnetic and mechanical properties In  $\text{FeXSIB}$  ( $X=\text{Cu,Zr,Co}$ ) amorphous alloys, *Archives of Materials Science and Engineering* 31/1 (2008) 25-28.
- [24] Ł. Madej, Z. Stokłosa, A. Chrobak, P. Kwapiński, J. Rasek, G. Haneczok, Magnetic properties of  $\text{Fe}_{76}\text{X}_2\text{Si}_8\text{B}_{14}$

- (X=Al, Cr, Mo) amorphous alloys Archives of Materials Science and Engineering 34/1 (2008) 9-13.
- [25] W.J. Boettinger, U.R. Kattner, K.-W. Moon, J.H. Perepezko, DTA and heat-flux DSC measurements of alloy melting and freezing, National Institute of Standards and Technology Special Publication 960-15 (2006).
- [26] PN - EN ISO 6507 - 1:2007.
- [27] W.S. Sun, T. Kulik, X.B. Liang, J. Ferenc, Thermal stability and magnetic properties of Co-Fe-Hf-Ti-Mo-B bulk metallic glass, Intermetallics 14 (2006) 1066-1068.
- [28] W.H. Wang, Roles of minor additions in formation and properties of bulk metallic glasses, Progress in Materials Science 52 (2007) 540-596.